Available online at www.sciencedirect.com

ScienceDirect

journal homepage: www.elsevier.com/locate/he

CFD simulation of CO_2 removal from hydrogen rich stream in a microchannel

*M.A. Makarem, M. Farsi**, M.R. Rahimpour**

Department of Chemical Engineering, Shiraz University, Shiraz, Iran

HIGHLIGHTS

- The CO_2 capture from hydrogen rich streams is simulated in T-Junction microchannel.
- The CFD simulation is used to investigate the fluid hydrodynamics and mass transfer.
- The continuity, Navier-Stokes, two phase transport, and reaction rate are coupled.
- The effects of gas and liquid flow rates and DEA concentration are investigated.

GRAPHICAL ABSTRACT

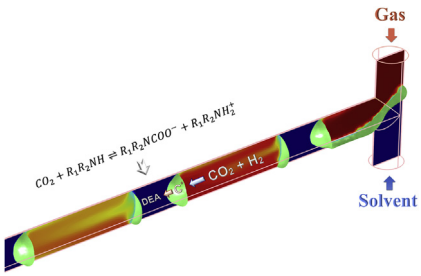

ARTICLE INFO

Article history:
Received 31 May 2020
Received in revised form
2 July 2020
Accepted 24 July 2020
Available online xxx

Keywords:
Microchannel
CFD Simulation
Hydrogen purification
Carbon dioxide capturing

ABSTRACT

The main object of this research is to perform computational fluid dynamics simulation of CO_2 capturing from hydrogen-rich streams by aqueous DEA solution in a T-Junction microchannel contactor with 250 μm diameter and 5 mm length at dynamic conditions. To develop a comprehensive mathematical framework to simulate the flow hydrodynamics and mass transfer characteristics of system, the continuity and Navier-Stokes equations, two phase transport, and reaction rate model are coupled in COMSOL Multiphysics software. The developed model is solved and the effects of gas and liquid velocities as well as amine concentration on the CO_2 absorption rate, hydrogen purification fraction, and flow hydrodynamic are investigated. The absorption process consists of CO_2 diffusion from bubble bulk toward the bubble boundary, CO_2 solubility in the liquid boundary, diffusion from the boundary into the liquid bulk, and reaction with the amine molecules. The results show that when the gas and liquid streams are mixed in the junction point to form a bubble, the gas cross-section area becomes narrow, and the fluid velocity increases due to the applied force on the bubble by the liquid layers. It appears that increasing the DEA concentration in the inlet from 5% to 20% increases hydrogen purification fraction from 42.3 to 66.4%, and up to 96.7% hydrogen purity is achieved by 20% aqueous solution of DEA.

* *Corresponding author.*
** *Corresponding author.*
E-mail addresses: farsi@shirazu.ac.ir (M. Farsi), rahimpor@shirazu.ac.ir (M.R. Rahimpour).

https://doi.org/10.1016/j.ijhydene.2020.07.221
0360-3199/

Please cite this article as: Makarem MA et al., CFD simulation of CO_2 removal from hydrogen rich stream in a microchannel, International Journal of Hydrogen Energy, https://doi.org/10.1016/j.ijhydene.2020.07.221

Introduction

Due to increasing energy demand in the world, reducing the nonrenewable energy resources and extreme environmental drawbacks, many researchers have focused on finding green, high density, and economic energy alternatives [1]. Between proposed resources, hydrogen is the most promising candidate for energy delivery due to broad flammability range, high ignition temperature with very low ignition energy, high diffusivity, and fast flame speed [2]. It is the most abundant element in the universe and its compounds are widely distributed in Earth's crust [3]. Industrially, it is used in the hydrocarbons upgrading units, ammonia, methanol, and dimethyl ether synthesis plants and Fischer-Tropsch process [4]. Hydrogen energy yield is around 120 kJ g^{-1}, which is two times more than the yield of conventional fossil fuels [5]. The possibility of applying various production routes and different feeds are other advantages of hydrogen over other resources. Although partial oxidation, steam reforming, and auto-thermal reforming of hydrocarbons and water hydrolysis are common routes to produce hydrogen, it can be obtained by purifying exhale streams of industrial plants such as tale and flare gases. Currently, around 150 billion cubic meters of tale and flare gases burn in the flares annually [6]. The flare gas in the conventional methanol unit contains 60% hydrogen and 25% CO_2 as the main impurity, and purified hydrogen could be recycled to the plant. Besides, in chemical plants that used hydrogen as feedstock, purification of hydrogen rich streams is critical.

Currently, the development of efficient chemical ad physical solvents to separate CO_2 from hydrogen-rich streams is an attractive topic from academic and industrial viewpoints. Traditionally, the application of alkanolamines for CO_2 removal in large scale channels and packed beds [7], bubble columns [8], and spray columns [9] is more popular. Smith experimented CO_2 separation from coal-derived synthesis gas using a chemical solvent in a pilot packed bed column [10]. They simulated the proposed process considering an equilibrium based model in the ASPEN Plus simulator. The results showed that capturing CO_2 at high temperatures reduces the syngas precooling requirements and increases the water and CO_2 concentrations in syngas. Sagar et al. simulated the CO_2 removal from hydrogen-rich syngas by the aqueous solution of MEA based on a non-equilibrium model [11]. They investigated the effect of gas and solvent flow rates and feed temperature on CO_2 absorption efficiency. The results showed that increasing the flow rate and temperature of solvent improve process efficiency. Sarkarzadeh et al. simulated and optimized an industrial hydrogen unit at steady state condition. The applied tray column to separate CO_2 by MEA was modeled based on the mass and energy balance equations considering an equilibrium model [12]. It was concluded that absorber efficiency plays the main role on the quality of produced hydrogen and the performance of next catalytic units. Dave et al. developed a feasible process to separate CO_2 from syngas using a physical solvent (DMEPEG) in the hydrogen unit [13]. The performance of applied solvent and used column were assessed considering a rate-based model. The CO_2 recovery from syngas and solvent saturation were 90.4% and 89% at the optimal condition, respectively.

Although tray columns and packed beds are widely used for CO_2 capture, one of the main challenges of such apparatus is low interfacial area per unit volume which results in a low mass transfer coefficient [14]. In this regard, different channel contractors with the larger interfacial area have been suggested for chemical and physical absorption of gases into liquids, especially for carbon capture. Practically, the channels with a diameter range of 1–100 μm are considered as microchannels, 100–1000 μm as minichannels, 1–6 mm as compact tubes, and upper than 6 mm as conventional contactors [15]. The micro and minichannels can improve the mass transfer coefficient up to 1000 times than conventional absorption columns and result in the lower capital cost when the plant capacity is below 50 MMSCFD [16]. In general, when the solvent and CO_2 react fast and absorption is controlled by diffusion, smaller channels are good candidates for CO_2 capturing [17]. Zhu et al. experimented solubility and absorption rate of CO_2 into the aqueous solution of MEA in a 400 × 600 μm microchannel [18]. Since CO_2 and MEA react fast with each other and the absorption is controlled by mass transfer limitations, the utilized microchannel were effective to capture CO_2 from the gas mixture. They concluded that increasing the volumetric gas to liquid ratio changed the flow hydrodynamics in the channel and increased the liquid-side mass transfer coefficient significantly. Ganapathy et al. experimented absorption of CO_2 into aqueous DEA solution in a microchannel with circular cross-section and analyzed the process by using a high-speed camera [19]. The results showed that CO_2 absorption by DEA in microchannels was more efficient compared to conventional apparatus. In a similar study, Lin et al. studied CO_2 absorption into aqueous mixtures of MDEA and DEA in a microchannel [20]. The results showed that the CO_2 absorption efficiency and the liquid side mass transfer coefficient increased by increasing DEA concentration and liquid flow rate, and decreased by increasing the gas flow rate.

Since the experimental investigation of CO_2 absorption in microchannels is difficult and complex, many researches have been conducted on the theoretical approaches. In general, the computational fluid dynamics (CFD) is an acceptable framework to investigate the fluid hydrodynamics and mass transfer characteristics in microchannels. Dong et al. simulated the CO_2 absorption by aqueous solutions of ethanol, NaOH, and MEA in a microchannel device [21]. They investigated the effects of bubble velocity and contact time on the mass transfer coefficient. It was concluded that the volumetric mass transfer coefficient of chemical absorption was 3–10 times more than that of physical absorption. Firuzi and Sadeghi used computational fluid dynamics to investigate the CO_2 solubility in MEA solution and mass transfer characteristics of the annular flow pattern in a microchannel [22]. Simulation results indicated that increasing the superficial gas and liquid velocities, operating temperature, and solvent concentration increased the rate of mass transfer from gas toward the liquid.

While many researches have been conducted on CO_2 separation from hydrogen-rich stream and application of microchannels in gas absorption separately, removing CO_2 from the mixture of hydrogen-rich stream in such channels has not yet been addressed both experimentally and theoretically. In this

Please cite this article as: Makarem MA et al., CFD simulation of CO_2 removal from hydrogen rich stream in a microchannel, International Journal of Hydrogen Energy, https://doi.org/10.1016/j.ijhydene.2020.07.221

regard, the main object of this research is to perform computational fluid dynamics simulation of CO_2 capture in a microchannel. In Section Reaction mechanism, the reaction mechanism of CO_2 and aqueous DEA solution and the considered rate expression are presented. Afterward, the simulation procedure and applied model are explained in detail in Section Simulation procedure. Ultimately, the simulation results and remarkable conclusions are explained in Sections Results and discussions and Conclusions, respectively.

Reaction mechanism

Carbon dioxide capture by the DEA solution comprises five steps including CO_2 transfer from gas bubble toward the bubble interface, CO_2 diffusion and solubility into the bubble boundary layer, CO_2 solubility, and diffusion in the liquid boundary layer, and CO_2 transfer toward the liquid bulk with chemical reaction with DEA molecules. According to the presented data in the literature, the reaction of CO_2 and DEA is reversible and carries out in two steps [23]. The first reaction is rate controlling and second order, while the second one is instantaneous. The kinetics of these reactions are as [24]:

$$CO_2 + (CH_2CH_2OH)_2NH \underset{k_2}{\overset{k_1}{\rightleftharpoons}} (CH_2CH_2OH)_2NH^+COO^- \quad (1)$$

$$(CH_2CH_2OH)_2NH^+COO^- + CH_2CH_2OHNH \xrightarrow{k_3} (CH_2CH_2OH)_2NCOO^- + CH_2CH_2OHNH_2^+ \quad (2)$$

By considering steady-state approximation to the zwitterions and assuming the negligible concentration of ions, the apparent rate of the reaction is explained as:

$$r = \frac{1.41}{1 + \frac{1180}{C_{DEA}}} C_{CO_2} \quad (3)$$

The reaction in the liquid phase is calculated by applying the enhancement factor, which allows replacement of the liquid side concentration with that of the interface as:

$$R_{CO_2} = E k_L a C_{CO_2} = \frac{E k_L a \, P_{CO_2}}{H} \quad (4)$$

By applying the rate equation, the enhancement factor can be explained as:

$$E = \sqrt{1 + \frac{D_{CO_2} k_{app} C_{DEA}}{k_L^2}} \quad (5)$$

The liquid side mass transfer coefficient is calculated as [25]:

$$k_L = 2\sqrt{\frac{D_{CO_2}}{\pi \tau_c}} \quad (6)$$

Simulation procedure

In this research, COMSOL Multiphysics software, which is a well-known simulation package for investigating the performance of microchannels, is used to simulate the CO_2 absorption process [26]. The considered approach to simulate the hydrodynamics and mass transfer characteristics of CO_2 absorption from the mixture of CO_2 and H_2 in isobaric and isothermal conditions consist of laminar flow model to estimate spatial flow velocity, two phase flow model to identify gas and liquid boundaries and mass transfer model to calculate the concentrations in both phases and applying the reaction.

Microchannel geometry

In this research, a circular T-Junction micro-structured channel with 250 μm diameter and 5 mm length is designed as a gas-liquid contactor. Fig. 1 shows the detailed schematic of the considered channel to separate CO_2 from the mixture of CO_2 and H_2 by aqueous DEA solution. In the simulated contactor, the horizontal channel is joined exactly to the middle of vertical one. The liquid is fed from the bottom of vertical channel, while the gas stream flows from the top. The applied gas and liquid streams are mixed at the junction point to form bubbles and flows in the horizontal channel. To perform computational fluid dynamics simulation of the process, the tetrahedral mesh distribution is applied on the channel considering symmetric boundary condition at channel depth. To apply a suitable mesh structure, the elements near the boundaries are supposed to be smaller compared to the channel body, especially when two channels are joined together. Indeed, the channel geometry has been divided into different sections in order to specify the mesh element size and distribution. Fig. 2 shows the applied meshing distribution on the channel.

Flow model

Laminar flow model

To investigate the fluid hydrodynamics and velocity profiles in the considered microchannel, the dynamic mass continuity and Navier-Stokes equations are considered as:

$$\frac{\partial \rho}{\partial t} + \nabla.(\rho \mathbf{u}) = 0 \quad (7)$$

$$\rho \frac{\partial \mathbf{u}}{\partial t} + \rho(\mathbf{u}.\nabla)\mathbf{u} = \nabla.\left[-p\mathbf{I} + \tau_f\right] + \mathbf{F} \quad (8)$$

where τ_f represents viscous stress tensor and explained as [27]:

$$\tau_f = 2\mu \mathbf{S} - \frac{2}{3}\mu(\nabla.\mathbf{u})\mathbf{I} \quad (9)$$

$$\mathbf{S} = \frac{1}{2}\left(\nabla \mathbf{u} + (\nabla \mathbf{u})^T\right) \quad (10)$$

Since the flow regime is assumed to be laminar, the turbulence terms in the Navier-Stokes equations are ignored and eliminated.

Two-phase flow model

To determine phase distribution in the microchannel, the dynamic transport equation is considered as:

Please cite this article as: Makarem MA et al., CFD simulation of CO_2 removal from hydrogen rich stream in a microchannel, International Journal of Hydrogen Energy, https://doi.org/10.1016/j.ijhydene.2020.07.221

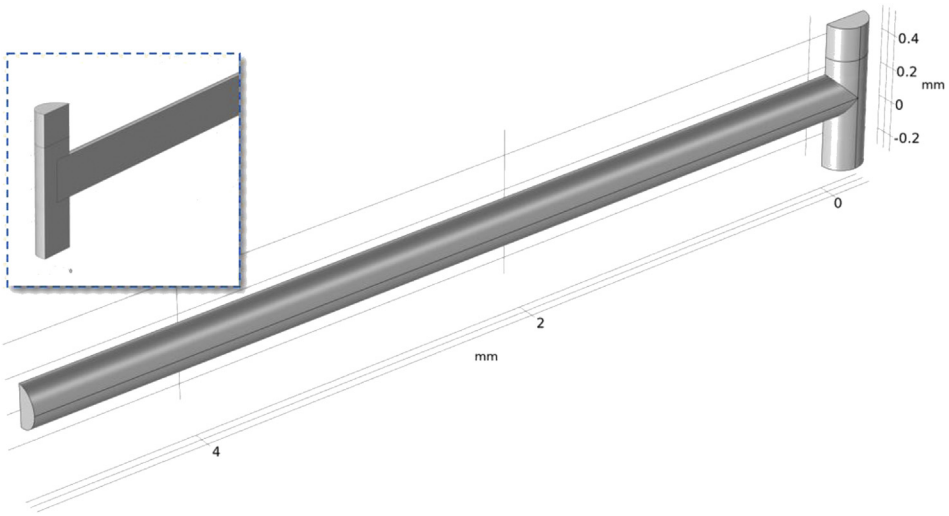

Fig. 1 – The geometry of simulated T-shaped microchannel.

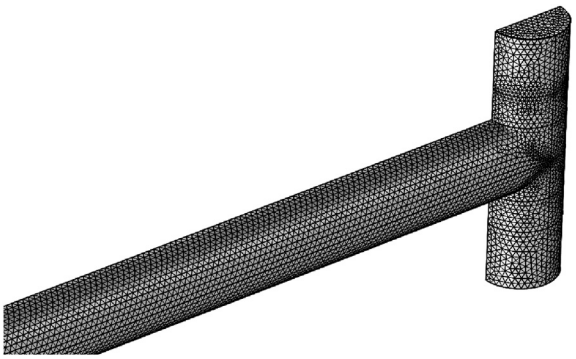

Fig. 2 – The applied Tetrahedral mesh distribution over the channel.

$$\frac{\partial \varphi}{\partial t} + \mathbf{u}.\nabla\varphi = \gamma\nabla.\left(\varepsilon\nabla\varphi - \varphi(1-\varphi)\frac{\nabla\varphi}{|\nabla\varphi|}\right) \quad (11)$$

where ε controls the interface thickness and its value is equal to the maximum mesh size in which the interface passes through.

Flow boundary conditions

The wetted wall boundary condition is applied on the channel to prohibit any mass penetration through the wall and permit to move the gas-liquid interface. Besides, it is responsible to adjust the contact angle between the wall and fluid interface frictional force as:

$$\mathbf{u}.\mathbf{n}_{wall} = 0 \quad (12)$$

$$\mathbf{F}_{\theta} = \sigma\delta(\mathbf{n}_{wall}.\mathbf{n} - \cos\theta_w) \quad (13)$$

$$\mathbf{F}_{fr} = -\frac{\mu}{\beta}\mathbf{u} \quad (14)$$

The inlet gas and liquid streams to the vertical part of channel are in single phase condition and the pressure of outlet stream from the horizontal part is assumed to be atmospheric.

Mass transfer model

To find the concentration gradient along the channel, the mass conservation equation is solved by considering both diffusion and convection mechanisms as:

$$\frac{\partial C_{CO_2}}{\partial t} + \nabla.(D_{CO_2}\nabla C_{CO_2}) + \mathbf{u}.\nabla c_{CO_2} = R_{CO_2} \quad (15)$$

Practically, CO_2 is absorbed by aqueous DEA solution and the volume of gas bubbles decreases along the channel. However the CO_2 concentration in the inlet gas is usually low in hydrogen-rich streams, and therefore, changes in the bubble size can be ignored [28]. On the other hand, since DEA and CO_2 reacts in the liquid phase and the inlet CO_2 to DEA molar ratio is low compared to the reaction stoichiometry, the CO_2 concentration in the liquid phase is negligible. In the outlet of the channel, the normal concentration gradient is assumed to be zero for both phases, which means free outward flow. To find the effect of operating parameters on the CO_2 absorption rate, the hydrogen purification fraction is defined as below.

$$\eta = \frac{C^{in}_{CO_2} - C^{out}_{CO_2}}{C^{in}_{CO_2}} \times 100\% \quad (16)$$

In this research to investigate the effects of DEA concentration on hydrogen purification fraction, DEA mass fraction is changed in the inlet liquid in each run. Table 1 shows the mass

Please cite this article as: Makarem MA et al., CFD simulation of CO_2 removal from hydrogen rich stream in a microchannel, International Journal of Hydrogen Energy, https://doi.org/10.1016/j.ijhydene.2020.07.221

diffusion coefficient, Henry's constant, viscosity, and density of inlet liquid at the considered DEA concentrations.

Results and discussions

In this section, the results of CO_2 absorption from the mixture of H_2 and CO_2 by the aqueous solution of DEA in the considered microchannel is presented at dynamic conditions. In general, the simulation results can be categorized into two main groups, i. e. flow hydrodynamics and mass transfer characteristics. Simulations are performed on a high-speed computer with an Intel Core i7 6850K processor running at 3.6 GH and using 32 GB of RAM.

Channel hydrodynamics

Fig. 3 illustrates the streamlines and velocity profile inside the considered microchannel. As mentioned before, the liquid stream feeds from the bottom of vertical channel, while the gas stream flows from the top. The inlet gas stream is bubbled into the liquid phase and flows along the horizontal part of microchannel. It appears that the fluid velocity increases along the radial direction and the maximum velocity is developed at the channel centerline. Since the gas stream is collapsed into bubbles and surrounded by the liquid medium in the horizontal part, the mean fluid velocity increases in this part of the microchannel up to three times more than the velocity of the inlet gas stream. On the other hand, the flow layers and the streamlines are a bit compressed and curved when the bubbles enter the horizontal channel.

Fig. 4 shows the bubble formation procedure and fluid velocity during the process run time. When the gas and liquid are mixed in the junction point and a bubble is formed, the gas cross-section area becomes narrow and the fluid velocity increases up to 2.5 m s^{-1}. Indeed, the applied force on the bubble by liquid layers pushes the bubble in the microchannel and increases the bubble velocity in the junction point. As can be seen, at the moment the bubble formation begins, the velocity is almost equal to the initial value, i.e. 8 cm s^{-1}.

Mass transfer characteristics

In general, the CO_2 molecules absorb into the liquid phase and react with DEA as gas bubbles move along the channel. Therefore, the residence time is one of the most important factors affecting purification percent. The residence time can be controlled by the fluid flow rate and channel length. Fig. 5 shows the hydrogen enrichment in the bubbles along the channel length at three different gas velocities 0.05, 0.07, and 0.09 m s^{-1}. As bubble flows along the microchannel, CO_2 is transferred toward the liquid and hydrogen concentration increases in the bubble. The maximum hydrogen concentration appears in the outgoing bubbles from the microchannel. In general, the CO_2 molecules are transferred from bubble bulk toward the bubble boundary and diffuse into the bubble boundary layer. Afterward, CO_2 is dissolved in the liquid boundary layer and then transferred toward the liquid bulk and reacts with DEA molecules. Therefore, the hydrogen concentration decreases along the radial direction of bubbles and maximum hydrogen concentration is developed close to the bubble boundary. Applying higher gas flow rates increases the length of formed bubbles and reduces the bubble residence time in the channel which changes the flow pattern from Taylor flow to bubbly or annular flow and reduces the mass transfer coefficient in the system [29]. On the other hand, in the considered system, increasing the gas flow rate decreases the CO_2 transfer rate from gas toward the liquid and results in lower hydrogen purification fraction.

Fig. 6 shows the effect of gas velocity in the range of 5–10 cm s^{-1} on hydrogen purification fraction and outlet CO_2 concentration in the outgoing bubble from the microchannel. It appears that increasing gas velocity from 5 to 10 cm s^{-1} decreases hydrogen purification fraction from 53.8% to 40.3% and increases carbon dioxide concentration in the outlet gas stream from 4.6 to 6.0%. In general, decreasing the gas velocity highly affects the process capacity, flow pattern, and hydrogen purification fraction and might change the profitability of the process in larger scales. Hence, since its effect on the purification fraction is not great, it is recommended to set the gas flow rate as high as possible in which the flow pattern stays in Taylor flow to achieve maximum mass transfer coefficient. Fig. 7 represents the effect of liquid velocity in the range of 1–6 cm s^{-1} on the hydrogen purification fraction and outlet CO_2 concentration in the outgoing bubble from the microchannel. Although increasing the liquid velocity decreases the resident time in the channel, it improves inner circulation in the liquid slugs and enhances the liquid-side mass transfer coefficient, which results in a higher mass transfer rate. It appears that increasing the liquid velocity from 1 to 6 cm s^{-1} increases hydrogen purification fraction from 39.8% to 53.7% and decreases CO_2 concentration in the outlet gas stream from 6.0 to 4.7%. Based on the presented data, when liquid velocity increases from 1 cm s^{-1}, the resident time reduction is comparable with mass transfer enhancement and hydrogen purification fraction is improved slightly. Increasing the liquid velocity to 6 cm s^{-1} leads to greater enhancements in the slope of hydrogen purity fraction profile. A similar observation is reported in experimental studies [20].

Fig. 8 presents the effect of DEA concentration on CO_2 capture from the gas stream in the range of 5–20 wt percent. In general, increasing the amine concentration enhances the rate of CO_2-DEA reaction and increases the mass transfer rate in the system. It appears that increasing the concentration of DEA in the inlet liquid from 5% to 20% increases the hydrogen purification fraction from 42.3 to 66.4%, and up to 96.7% hydrogen purity is achieved by 20% aqueous solution of DEA. Fig. 9 presents the effect of DEA concentration on the reaction

Table 1 – DEA solutions specifications [38–41].

w %	C_{DEA} (mol m^{-3})	ρ (kg m^{-3})	μ_{DEA} (mPa s^{-1})	D_{CO2} (m^2 s^{-1})	H_{CO2} (Pa.m^3 mol^{-1})
5	474.76	1001.31	1.09	1.64×10^{-9}	3268.61
10	949.52	1005.56	1.23	1.46×10^{-9}	3320.19
15	1424.29	1009.85	1.38	1.27×10^{-9}	3371.76
20	1899.05	1014.17	1.53	1.08×10^{-9}	3423.34

Please cite this article as: Makarem MA et al., CFD simulation of CO_2 removal from hydrogen rich stream in a microchannel, International Journal of Hydrogen Energy, https://doi.org/10.1016/j.ijhydene.2020.07.221

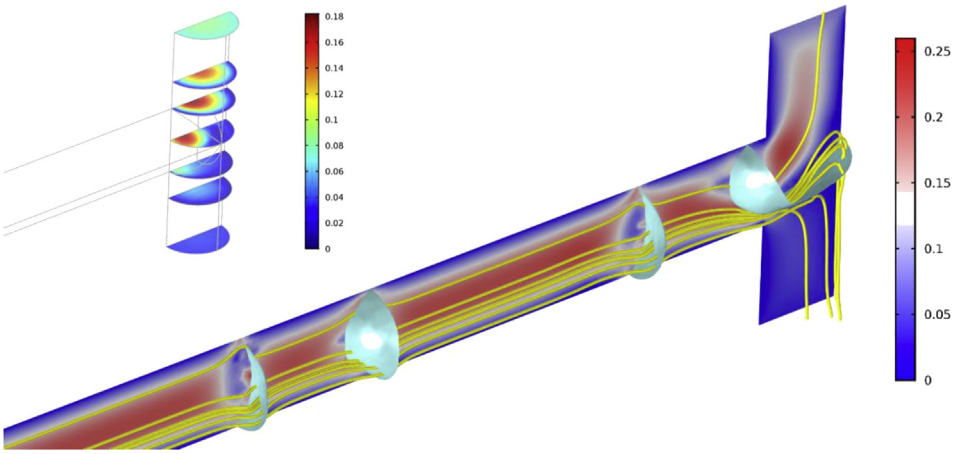

Fig. 3 – Velocity magnitude and stream lines profile at $u_G = 0.08$ m s^{-1}, $u_L = 0.03$ m s^{-1} and DEA mass fraction 5%.

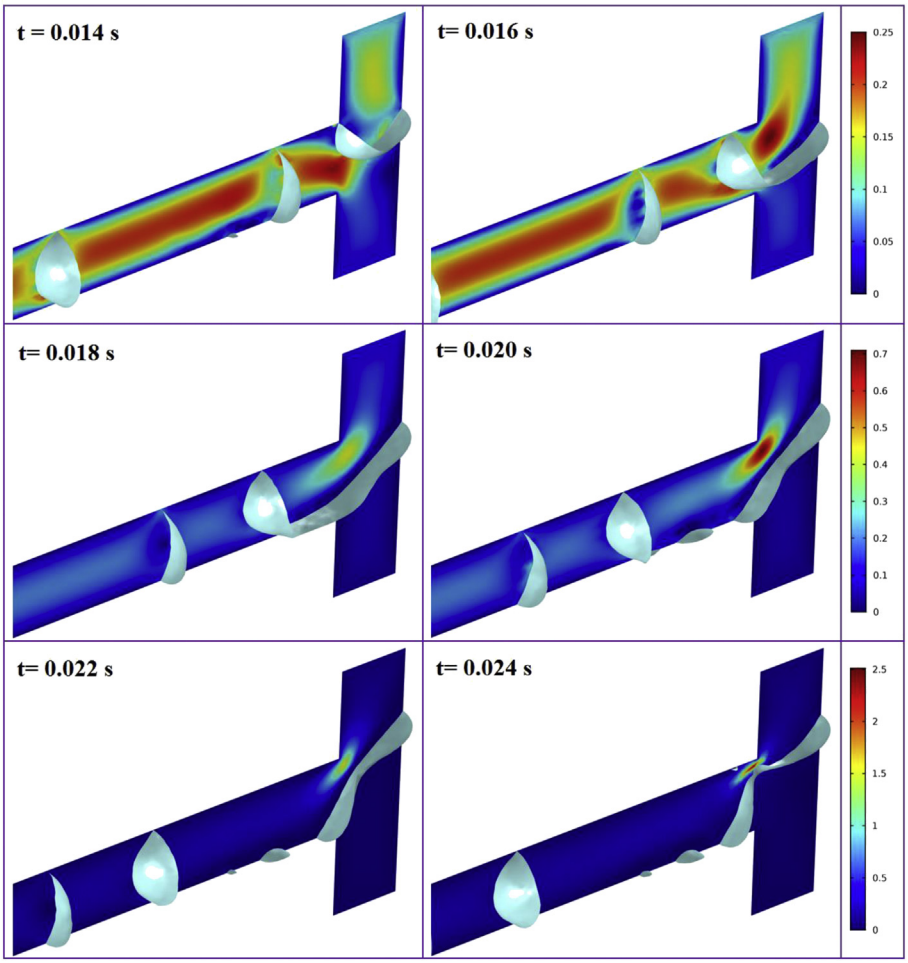

Fig. 4 – Bubble formation and flow velocity profile at $u_G = 0.08$ m s^{-1}, $u_L = 0.03$ m s^{-1} and DEA mass fraction 5%.

rate along the microchannel. Based on the simulation results, the maximum reaction rate is developed at the entrance of horizontal part of the channel where CO_2 and DEA concentrations are at their maximum values. As the gas and liquid phases flow along the channel, carbon dioxide is absorbed and CO_2 content in the bubble and DEA concentration in the liquid phase decrease gradually. Decreasing CO_2 and DEA concentrations reduce the reaction rate along the channel. Besides, increasing the amine solution concentration from 5% to 10%, enhances the mean reaction rate by 50% while changing the concentration from 15% to 20% only enhances the mean reaction rate by 10%.

Please cite this article as: Makarem MA et al., CFD simulation of CO_2 removal from hydrogen rich stream in a microchannel, International Journal of Hydrogen Energy, https://doi.org/10.1016/j.ijhydene.2020.07.221

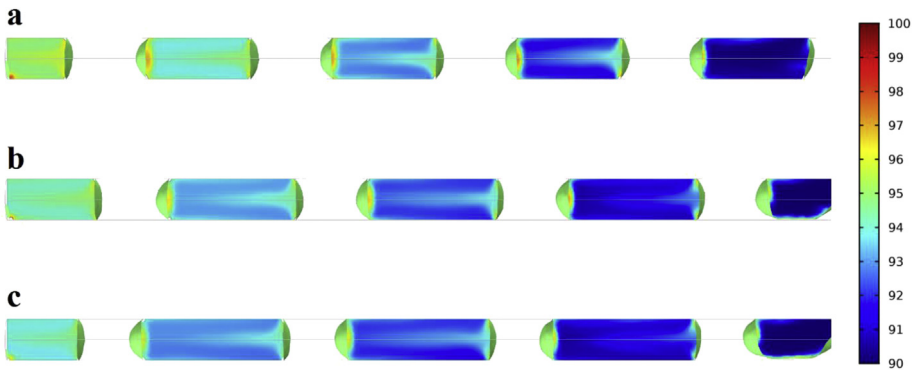

Fig. 5 – Hydrogen purity enrichment through the microchannel at DEA mass fraction 5%, $u_L = 3$ cm s^{-1} (a) $u_G = 0.05$ m s^{-1}, (b) $u_G = 0.07$ m s^{-1} (c) $u_G = 0.09$ m s^{-1}.

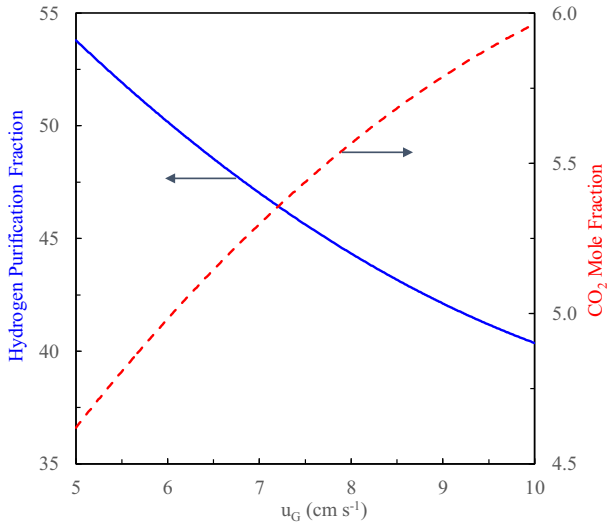

Fig. 6 – Effect of gas velocity on hydrogen purification fraction and CO_2 concentration in gas bubbles at DEA mass fraction 5%, $u_L = 0.03$ m s^{-1}.

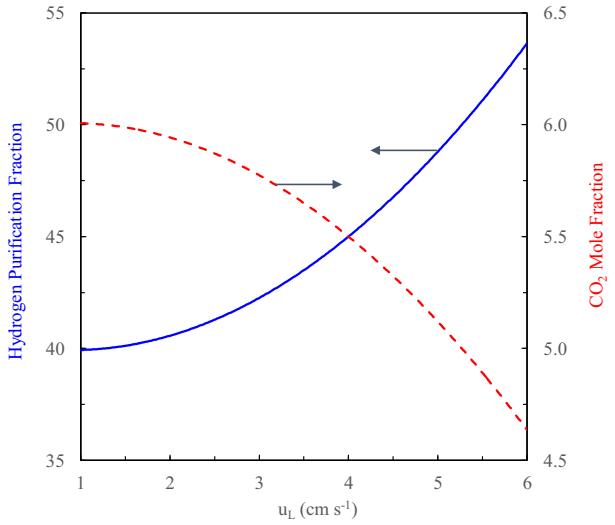

Fig. 7 – Effect of inlet liquid velocity on hydrogen purification fraction and CO_2 concentration in gas bubbles at DEA mass fraction 5%, $u_g = 0.09$ m s^{-1}.

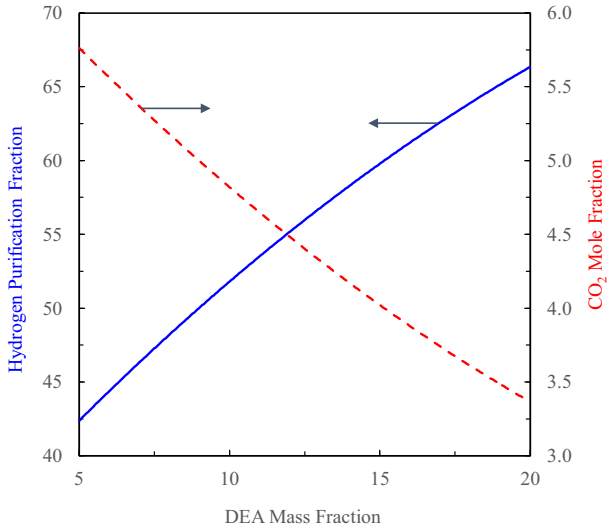

Fig. 8 – Effect of DEA concentration on hydrogen purification fraction and CO_2 concentration in gas bubbles at $u_g = 0.09$ m s^{-1}, $u_L = 3$ m s^{-1}.

Industrialization and application extension

In general, microchannels could be used in absorption processes as high-performance contactors. Since the interfacial area is highly increased by microchannels, these apparatus can be utilized to separate CO_2, sulfide gases and other impurities from gas mixtures. In general, hydrogen sulfide is another impurity in the gas streams that affects gas specifications and can be effectively absorbed by alkanolamines in microchannels more efficiently than conventional contactors [30–32]. On the other hand, when it is essential to use solid absorbers or catalysts, microchannels can increase contacting area as well [33]. In this regard packed bed micro-reactors can be designed by packing the catalyst powders in the channels or specifically create microchannels in the bulk of catalyst. However, pressure drop and energy dissipation is one of the main challenges in these structures and must well

Please cite this article as: Makarem MA et al., CFD simulation of CO_2 removal from hydrogen rich stream in a microchannel, International Journal of Hydrogen Energy, https://doi.org/10.1016/j.ijhydene.2020.07.221

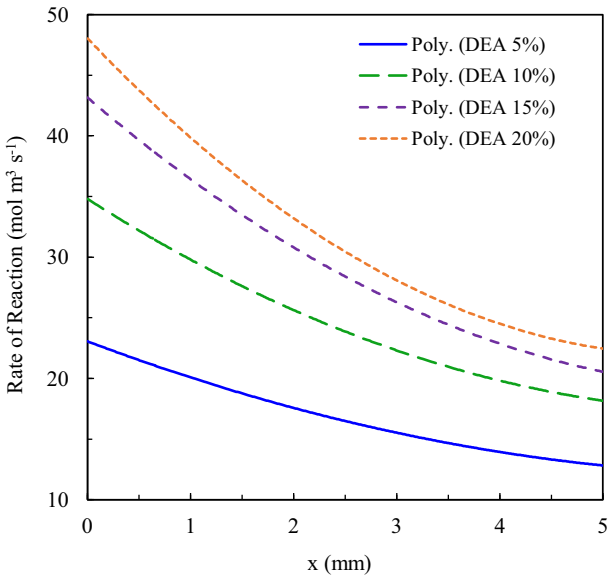

Fig. 9 – Rate of carbon dioxide reaction along the channel at different DEA concentrations at $u_g = 0.09$ m s^{-1}, $u_L = 3$ m s^{-1}.

be considered in industrial scales [34,35]. From an industrial viewpoint, to make the microchannels useable in large scale absorption processes, scaling up is necessary. The most popular method to scale up of small channels is parallel numbering up, which means utilizing separate channels parallel with each other. The performance and efficiency of parallel combination is highly related to the fluid distribution at the entrance of the structure [36]. Although the scaled-up microchannels show a reduction in the overall mass transfer coefficient compared to single channels, based on the presented data in the literature, the yield of such micro-structured contactors is still 1–3 orders of magnitude higher than conventional gas-liquid absorbers, including packed beds [37].

Conclusions

In this research, the computational fluid dynamics simulation of CO_2 capturing from hydrogen-rich streams in a microchannel contactor was performed by coupling the continuity and Navier-Stokes, two phase transport, mass transfer, and reaction rate models. The COMSOL Multiphysics software was used to simulate the performance of microchannels considering tetrahedral mesh distribution. The simulation results showed that since the gas stream was collapsed into bubbles and surrounded by the liquid medium in the horizontal part, the mean fluid velocity increased in this part up to three times more than the velocity of inlet gas stream. Due to mass transfer resistance in the gas and liquid phases, the hydrogen concentration decreased along the radial direction of bubbles and maximum hydrogen concentration was developed close to the bubble boundary. The residence time was found as one of the most important factors affecting purification percent. It appeared that increasing the gas velocity from 5 to 10 cm s^{-1} decreased the hydrogen purification fraction from 53.8% to 40.3% and increased CO_2 concentration in the outlet gas stream from 4.6 to 6.0%. Besides, increasing the liquid velocity from 1 to 6 cm s^{-1} increased the hydrogen purification fraction and decreased CO_2 concentration by 13.9% and 23.1%, respectively.

Declaration of competing interest

The authors whose names are listed in the manuscript certify that they declare no conflict of interest.

Nomenclatures

a	Interfacial area (m^2)
c	Concentration (mol m^{-3})
D	Diffusion coefficient (m^2 s^{-1})
E	Enhancement factor
$\mathbf{F}$	Volume force vector (N m^{-3})
H	Henry's constant (Pa m^3 mol^{-1})
i	Gas-liquid interface
k	Reaction rate constant
k_L	Liquid side mass transfer coefficient (m s^{-1})
$\mathbf{n}$	Normal vector
p	Pressure (Pa)
R	Reaction rate expression (mol m^{-3} s^{-1})
$\mathbf{S}$	Strain rate tensor
t	Time (s)
$\mathbf{u}$	Velocity vector (m s^{-1})
w	Mass fraction
x	Channel length (m)
y	Mole fraction

Greek Letter

β	Slip length (m)
μ	Dynamic viscosity (Pa s^{-1})
γ	Reinitialization parameter (m s^{-1})
ε	Interface controlling parameter (m)
φ	Volume fraction
τ_c	Residence time (s)
τ_f	Viscous stress tensor (Pa)
ρ	Density (kg m^{-3})
θ_w	Contact angel (rad)
η	Hydrogen purification fraction

REFERENCES

[1] Nigam PS, Singh A. Production of liquid biofuels from renewable resources. Prog Energy Combust Sci 2011;37:52–68.
[2] Abe J, Popoola A, Ajenifuja E, Popoola O. Hydrogen energy, economy and storage: review and recommendation. Int J Hydrogen Energy 2019;44:15072–86.
[3] Baykara SZ. Hydrogen: a brief overview on its sources, production and environmental impact. Int J Hydrogen Energy 2018;43:10605–14.

Please cite this article as: Makarem MA et al., CFD simulation of CO_2 removal from hydrogen rich stream in a microchannel, International Journal of Hydrogen Energy, https://doi.org/10.1016/j.ijhydene.2020.07.221

[4] Sharma Ghoshal. Hydrogen the future transportation fuel: from production to applications. Renew Sustain Energy Rev 2015;43:1151–8.
[5] Balat M. Potential importance of hydrogen as a future solution to environmental and transportation problems. Int J Hydrogen Energy 2008;33:4013–29.
[6] Khanipour M, Mirvakili A, Bakhtyari A, Farniaei M, Rahimpour MR. A membrane-assisted hydrogen and carbon oxides separation from flare gas and recovery to a commercial methanol reactor. Int J Hydrogen Energy 2020;45:7386–400.
[7] Aboudheir A, Tontiwachwuthikul P, Idem R. Rigorous model for predicting the behavior of CO_2 absorption into AMP in packed-bed absorption columns. Ind Eng Chem Res 2006;45:2553–7.
[8] La Rubia MD, García-Abuín A, Gómez-Díaz D, Navaza JM. Interfacial area and mass transfer in carbon dioxide absorption in TEA aqueous solutions in a bubble column reactor. Chem Eng Process 2010;49:852–8.
[9] Tamhankar Y, King B, Whiteley J, Cai T, McCarley K, Resetarits M, et al. Spray absorption of CO_2 into monoethanolamine: mass transfer coefficients, dropsize, and planar surface area. Chem Eng Res Des 2015;104:376–89.
[10] Smith KH, Anderson CJ, Tao W, Endo K, Mumford KA, Kentish SE, et al. Pre-combustion capture of CO_2—results from solvent absorption pilot plant trials using 30 wt% potassium carbonate and boric acid promoted potassium carbonate solvent. Int J Greenh Gas Con 2012;10:64–73.
[11] Sourav S. Production of hydrogen enriched SYN-gas by absorption method. 2012.
[12] Sarkarzadeh M, Farsi M, Rahimpour M. Modeling and optimization of an industrial hydrogen unit in a crude oil refinery. Int J Hydrogen Energy 2019;44:10415–26.
[13] Dave A, Dave M, Huang Y, Rezvani S, Hewitt N. Process design for CO2 absorption from syngas using physical solvent DMEPEG. Int J Greenh Gas Con 2016;49:436–48.
[14] Charpentier J-C. Mass-transfer rates in gas-liquid absorbers and reactors. In: Advances in chemical engineering. Elsevier; 1981. p. 1–133.
[15] Mehendale S, Jacobi A, Shah R. Fluid flow and heat transfer at micro-and meso-scales with application to heat exchanger design. Appl Mech Rev 2000;53:175–93.
[16] Yang Z, Khan TS, Alshehhi M, AlWahedi YF. Economic assessment of carbon capture by minichannel absorbers. AIChE J 2018;64:620–31.
[17] Chunbo Y, Guangwen C, Quan Y. Process characteristics of CO_2 absorption by aqueous monoethanolamine in a microchannel reactor. Chin J Chem Eng 2012;20:111–9.
[18] Zhu C, Li C, Gao X, Ma Y, Liu D. Taylor flow and mass transfer of CO_2 chemical absorption into MEA aqueous solutions in a T-junction microchannel. Int J Heat Mass Tran 2014;73:492–9.
[19] Ganapathy H, Shooshtari A, Dessiatoun S, Alshehhi M, Ohadi M. Fluid flow and mass transfer characteristics of enhanced CO_2 capture in a minichannel reactor. Appl Energy 2014;119:43–56.
[20] Lin G, Jiang S, Zhu C, Fu T, Ma Y. Mass-transfer characteristics of CO_2 absorption into aqueous solutions of N-methyldiethanolamine+ diethanolamine in a T-junction microchannel. ACS Sustainable Chem Eng 2019;7:4368–75.
[21] Dong R, Chu D, Jin Z. Numerical simulation of the mass transfer process of CO_2 absorption by different solutions in a microchannel. Can J Chem Eng 2020:1–17. https://doi.org/10.1002/cjce.23781.
[22] Firuzi S, Sadeghi R. Simulation of carbon dioxide absorption process by aqueous monoethanolamine in a microchannel in annular flow pattern. Microfluid Nanofluidics 2018;22:109.
[23] Hikita, et al. The kinetics of reactions of carbon dioxide with monoethanolamine, diethanolamine and triethanolamine by a rapid mixing method. Chem Eng J 1977;13:7–12.
[24] Aboudheir, et al. Kinetics ofthe reactive absorption of carbon dioxide in high CO_2-loaded, concentrated aqueous monoethanolamine solutions. Chem Eng Sci 2003;58:5195–210.
[25] Nieves-Remacha MJ, Kulkarni AA, Jensen KF. Gas–liquid flow and mass transfer in an advanced-flow reactor. Ind Eng Chem Res 2013;52:8996–9010.
[26] Turgay MB, Yazıcıoğlu AG. Numerical simulation of fluid flow and heat transfer in a trapezoidal microchannel with COMSOL multiphysics: a case study. Numer Heat Tran, Part A: Applications 2018;73:332–46.
[27] Stokes GG. On the theories of the internal friction of fluids in motion, and of the equilibrium and motion of elastic solids. Trans Cambridge Philos Soc 1880;8.
[28] Ganapathy H, Al-Hajri E, Ohadi M. Mass transfer characteristics of gas–liquid absorption during Taylor flow in mini/microchannel reactors. Chem Eng Sci 2013;101:69–80.
[29] Haase S, Murzin DY, Salmi T. Review on hydrodynamics and mass transfer in minichannel wall reactors with gas–liquid Taylor flow. Chem Eng Res Des 2016;113:304–29.
[30] Shah MS, Tsapatsis M, Siepmann JI. Hydrogen sulfide capture: from absorption in polar liquids to oxide, zeolite, and metal–organic framework adsorbents and membranes. Chem Rev 2017;117:9755–803.
[31] Pan M-Y, Li T, Zhou Y, Qian Z, Shao L, Wang J-X, et al. Selective absorption of H2S from a gas mixture with CO2 in a microporous tube-in-tube microchannel reactor. Chem Eng Process 2015;95:135–42.
[32] Su H, Wang S, Niu H, Pan L, Wang A, Hu Y. Mass transfer characteristics of H2S absorption from gaseous mixture into methyldiethanolamine solution in a T-junction microchannel. Separ Purif Technol 2010;72:326–34.
[33] Hessel V, Angeli P, Gavriilidis A, Löwe H. Gas– liquid and gas– liquid– solid microstructured reactors: contacting principles and applications. Ind Eng Chem Res 2005;44:9750–69.
[34] Losey MW, Schmidt MA, Jensen KF. Microfabricated multiphase packed-bed reactors: characterization of mass transfer and reactions. Ind Eng Chem Res 2001;40:2555–62.
[35] Losey MW, Jackman RJ, Firebaugh SL, Schmidt MA, Jensen KF. Design and fabrication of microfluidic devices for multiphase mixing and reaction. J Microelectromech Syst 2002;11:709–17.
[36] Haase S, Bauer T, Lange R. Numbering-up of mini-and microchannel contactors and reactors. Chim Oggi Chem Today 2015;33:2.
[37] Ganapathy H, Steinmayer S, Shooshtari A, Dessiatoun S, Ohadi MM, Alshehhi M. Process intensification characteristics of a microreactor absorber for enhanced CO_2 capture. Appl Energy 2016;162:416–27.
[38] Ganapathy H, Shooshtari A, Dessiatoun S, Ohadi M, Alshehhi M. Hydrodynamics and mass transfer performance of a microreactor for enhanced gas separation processes. Chem Eng J 2015;266:258–70.
[39] Kohl A, Nielsen R. Gas purification. 5th ed. Houston: Gulf Publishing Company; 1997.
[40] Versteeg GF, Van Swaaij WP. Solubility and diffusivity of acid gases (carbon dioxide, nitrous oxide) in aqueous alkanolamine solutions. J Chem Eng Data 1988;33:29–34.
[41] Browning GJ, Weiland RH. Physical solubility of carbon dioxide in aqueous alkanolamines via nitrous oxide analogy. J Chem Eng Data 1994;39:817–22.

Please cite this article as: Makarem MA et al., CFD simulation of CO_2 removal from hydrogen rich stream in a microchannel, International Journal of Hydrogen Energy, https://doi.org/10.1016/j.ijhydene.2020.07.221